

OPEN ACCESS

EDITED BY Antonio Caggiano, University of Genoa, Italy

REVIEWED BY
Tuo Huang,
Changsha University of Science and
Technology, China
Xiaocun Liu,
Shandong Jiaotong University, China

*CORRESPONDENCE Hongliu Rong, ⋈ 836490541@qq.com

RECEIVED 01 September 2025 ACCEPTED 13 October 2025 PUBLISHED 28 October 2025

CITATION

Yi Q, Zhang Z, Tan S, Peng C and Rong H (2025) Study of the modification mechanism and high-temperature rheological properties of OMMT/SBS-modified asphalt. Front. Mater. 12:1681616. doi: 10.3389/fmats.2025.1681616

COPYRIGHT

© 2025 Yi, Zhang, Tan, Peng and Rong. This is an open-access article distributed under the terms of the Creative Commons Attribution License (CC BY). The use, distribution or reproduction in other forums is permitted, provided the original author(s) and the copyright owner(s) are credited and that the original publication in this journal is cited, in accordance with accepted academic practice. No use, distribution or reproduction is permitted which does not comply with these terms.

Study of the modification mechanism and high-temperature rheological properties of OMMT/SBS-modified asphalt

Qiang Yi¹, Zhenghao Zhang², Shengrui Tan³, Chunhong Peng³ and Hongliu Rong³*

¹Guangxi Jiaotou Technology Co., Ltd., Nanning, Guangxi, China, ²Guangxi Special Geology Highway Safety Technology Innovation Center, Nanning, China, ³School of Civil Engineering and Architecture, Guangxi University, Nanning, Guangxi, China

This study systematically investigates the effects of two types of organic montmorillonite (OMMT-F and OMMT-C) on the physical and high-temperature properties of styrene-butadiene-styrene (SBS) modified asphalt to clarify the underlying modification mechanism. Through a combination of physical tests, Dynamic Shear Rheometer (DSR) analysis, Fluorescence Microscopy (FM), Fourier-Transform Infrared Spectroscopy (FTIR), and Atomic Force Microscopy (AFM), the results show that while OMMT content below 3% does not significantly impact flexibility, a 5% content of OMMT-F reduces penetration and ductility more severely than OMMT-C. Both OMMT types enhance hightemperature performance, as evidenced by an increased softening point and rutting factor, with FM revealing that OMMT promotes asphaltene agglomeration and AFM identifying a reinforcing honeycomb structure on the asphalt surface. FTIR analysis confirms that this modification is primarily a physical process. Collectively, these findings provide a comprehensive microscopiclevel comparison of OMMT types, offering valuable insights for optimizing SBS modified asphalt and presenting significant research value and practical implications for pavement engineering.

KEYWORDS

asphalt, OMMT, SBS, rheological property, FTIR, AFM

1 Introduction

The swift expansion of expressways and the substantial increase in traffic flow in China have prompted a demand for elevated standards in road durability, performance, environmental sustainability, and related aspects. Conventional polymer-modified asphalt, including materials like SBS, SBR, and rubber asphalt, has gained widespread adoption due to its commendable attributes such as superior high and low-temperature performance, water resistance, and fatigue resistance (Wang et al., 2013; Hou et al., 2017; Larsen et al., 2009; Iskender et al., 2012; Park et al., 2009), resulting in notable practical achievements. However, challenges persist, notably the intricate modification procedures and suboptimal compatibility with asphalt binders (Larsen et al., 2009; Liu et al., 2014), emerging as the primary technical impediment hindering the advancement of polymer-modified asphalt.

Nanomaterials find widespread application as modifiers in asphalt due to their diminutive particle size (1 nm-100 nm), expansive specific surface area, and favorable compatibility with asphalt (Zhang Shuai, 2020). Among these nanomaterials, nanoclay, categorized as a layered silicate, encompasses montmorillonite (MMT), vermiculite (VMT), kaolinite clay (KC), and others, characterized by particle sizes ranging from 200 nm to 400 nm (Ren Xiaoyu et al., 2020). Nano-clay exhibits the potential for intercalation or exfoliation upon blending with an asphalt binder (Wen-jun, 2013). Recent research indicates that the incorporation of nano-montmorillonite enhances the rutting resistance, fatigue resistance, aging resistance, and storage stability of the asphalt binder (Xiong Hui, 2020). Notably, compared to montmorillonite (MMT), organic montmorillonite (OMMT) demonstrates superior performance by forming an exfoliated structure in the asphalt binder (Ll Bo et al., 2017). Furthermore, nano-clay significantly improves the dispersion of polymers within the asphalt binder, resulting in noteworthy economic and technical benefits (Jasso et al., 2012). The development of nano-modified asphalt pavement materials emerges as a pivotal research direction in the field of road engineering (Transport, 2013). This avenue holds considerable promise, given its high potential for widespread adoption and its positive outlook for future development.

In recent years, both domestic and international researchers have conducted extensive investigations into asphalt modified with nano-clay. The preparation of nano-clay modified asphalt involved a melt blending process, with the dispersion of nano-clay in the asphalt binder analyzed using X-ray diffractometry (XRD). The findings revealed that montmorillonite-modified asphalt exhibited an intercalation structure, while organic montmorillonitemodified asphalt demonstrated an exfoliated structure (Yu et al., 2007). The incorporation of an appropriate quantity of organic montmorillonite markedly enhances the compatibility between styrene-butadiene-styrene (SBS) and the base asphalt. In a study by Shah et al., organic montmorillonite (OMMT) was introduced into SBS-modified asphalt, revealing that OMMT facilitates the achievement of improved physical and rheological properties when the clay is dispersed on a nanometer scale within the modified asphalt (Shah and Mir, 2020). Furthermore, Wang et al. identified that the OMMT modifier effectively addresses the deficiency of poor rutting resistance observed in bio-asphalt at elevated temperatures (Chao et al., 2022). Jahromi et al. discovered that, beyond enhancing the rheological properties of nano-clay modified asphalt, the inclusion of organic montmorillonite (OMMT) also enhances asphalt elastic modulus G and aging resistance (Jahromi and Khodaii, 2009). Focusing on storage stability, Yu et al. conducted a static storage test to evaluate the storage stability of both montmorillonite (MMT) and OMMT-modified asphalt. The study revealed that the storage stability of asphalt modified with MMT or OMMT remains highly stable when the clay content is below 3 wt%. Moreover, the storage stability of OMMT-modified asphalt surpasses that of MMT-modified asphalt, a finding supported by X-ray diffraction (XRD) testing. The presence of mostly exfoliated structures in OMMT-modified asphalt during modification suggests superior compatibility and dispersion ability with the base asphalt compared to MMT (Yu et al., 2007). In Tan et al.'s investigation, organic montmorillonite (OMMT) was introduced into crumb

rubber modified asphalt (CRMA), revealing that the modified asphalt with 3% and 4% OMMT content exhibited the most favorable storage stability (Tan et al., 2020). Ke et al. delved into the performance of styrene-ethylene-butadiene-styrene copolymer (SEBS)/OMMT-modified asphalt, highlighting OMMT's dual impact of enhancing high-temperature performance and promoting increased interaction between SEBS and asphalt molecules. This interaction improved the overall compatibility between SEBS and asphalt, consequently leading to a substantial enhancement in the hot storage stability of SEBS-modified asphalt (Yunbin et al., 2022). In the context of aging resistance, Zhang H. et al. (2011), Zhang et al. (2012), Zhang et al. (2013) and Zhang et al. (2014) used atomic force microscopy (AFM), X-ray diffraction (XRD), and Fourier transform infrared spectroscopy (FTIR) to study the microstructural changes of base asphalt and clay modified asphalt before and after aging. The results showed that FTIR and XRD showed that OMMT/SBS modified asphalt formed an intercalation structure, and the matrix stiffness of the asphalt increased after short-term aging. The AFM morphology gradually transitioned to single-phase with aging. OMMT can effectively prevent singlephase changes, indicating that OMMT/SBS modified asphalt has good UV aging resistance. However, the inclusion of layered clay effectively mitigates this phenomenon, underscoring the superior anti-aging performance of clay-modified asphalt. Furthermore, the introduction of organic montmorillonite (OMMT) serves to prevent the rupture of molecular bonds in asphalt by absorbing specific ultraviolet solar energy. This absorption mechanism contributes to enhancing the asphalt's resistance to ultraviolet aging (Wang et al., 2019). Liu et al. have substantiated this claim. Through Fourier Transform Infrared (FTIR) testing of modified asphalt before and after aging, coupled with an assessment using functional group indices to scrutinize the aging performance at a microscopic level, it was observed that the incorporation of organic montmorillonite (OMMT) markedly enhances the ultraviolet aging resistance of Sasobit warm mix asphalt. This finding serves to advance the potential application of Warm Mix Asphalt (WMA) in regions characterized by intense ultraviolet exposure (Liu et al., 2021). Lu et al. (2018) compared the effects of naphthenic oil and OMMT on the performance of SBS modified asphalt. The results show that both OMMT and naphthenic oil can improve the storage stability of SBS modified asphalt. OMMT deteriorates low-temperature performance, reduces high-temperature viscosity, and the high-temperature sensitivity reflected by softening point and rutting factor increases with the addition of OMMT (Crucho et al., 2019).

In summary, existing research on organic montmorillonite (OMMT) modified asphalt primarily focuses on investigating its rheological properties, storage stability, and anti-aging performance. These studies collectively validate the positive modification effects of OMMT, providing valuable insights for further exploration. However, there remains a gap in understanding the micromechanism underlying OMMT-modified asphalt, necessitating a more comprehensive qualitative and quantitative analysis of its modification mechanism. Building upon this context, the current study aims to investigate the traditional performance aspects of OMMT-modified asphalt. High-temperature rheological properties were assessed using a Dynamic Shear Rheometer (DSR), while Fourier Transform Infrared Spectroscopy (FTIR)

TABLE 1 Basic properties of SBS modified asphalt.

Penetration (25 °C, 100 g, 5 s)/0.1 mm	Ductility (5 cm/min, 5 °C)/cm	Softening point/°C	RTFOT (163 °C, 85 min)				
			Mass /%	Penetration ratio/%	10 °C Ductility/cm		
58.5	39.2	80.3	0.08	75	30		

was utilized for qualitative analysis of characteristic peaks and functional groups. Furthermore, a correlation between OMMT content and characteristic functional group indices was established to quantitatively determine OMMT content in modified asphalt. Additionally, Atomic Force Microscope (AFM) technology was employed to explore the impact of OMMT nano-modified materials on the micro-surface morphology of asphalt. This investigation aims to elucidate the micro-modification mechanism and identify factors contributing to the performance enhancement of OMMT-modified asphalt.

2 Materials and methods

2.1 Materials

2.1.1 SBS modified asphalt

This paper used a SBS modified asphalt as the reference asphalt. The selected SBS modified asphalt is prepared by high-speed shear mixing of SK 90# base asphalt and 5 %SBS modifier at 180 °C. Its main technical indicators are shown in Table 1. The testing process is mainly based on the "Standard Test Methods of Bitumen and Bituminous Mixtures for Highway Engineering " (JTG E20-2011) (Zhao et al., 2016; Sun et al., 2014).

2.1.2 Nano-clay modified materials

With the development of the production process, the particle size of layered clay is more refined in recent years. Some particles have reached a few micrometers or even smaller. However, there is no research to demonstrate how the particle size affects the performance of modified asphalt.

For this reason, two kinds of nano-clay (montmorillonite modifier) with different particle sizes were selected for study, in which the content of MMT was more than 95%. In order to improve the compatibility with asphalt binder, montmorillonite was modified by quaternary ammonium salt intercalation agent to prepare OMMT (Xiao and Zhang, 2017), which was recorded as OMMT-C (\geq 200 mesh) and OMMT-F (\geq 325 mesh), in which the specific gravity of OMMT-C and OMMT-F were 1.68 g/cm3 and 1.72 g/cm3, respectively. The chemical composition of different nano-clays is shown in Table 2.

Meanwhile, the microstructures of the two kinds of nanoclays were characterized by scanning electron microscopy (SEM), respectively, and the results are shown in Figure 1. It is evident from the SEM images that both materials have a lamellar structure. The microstructures of OMMT-C and OMMT-F are similar,

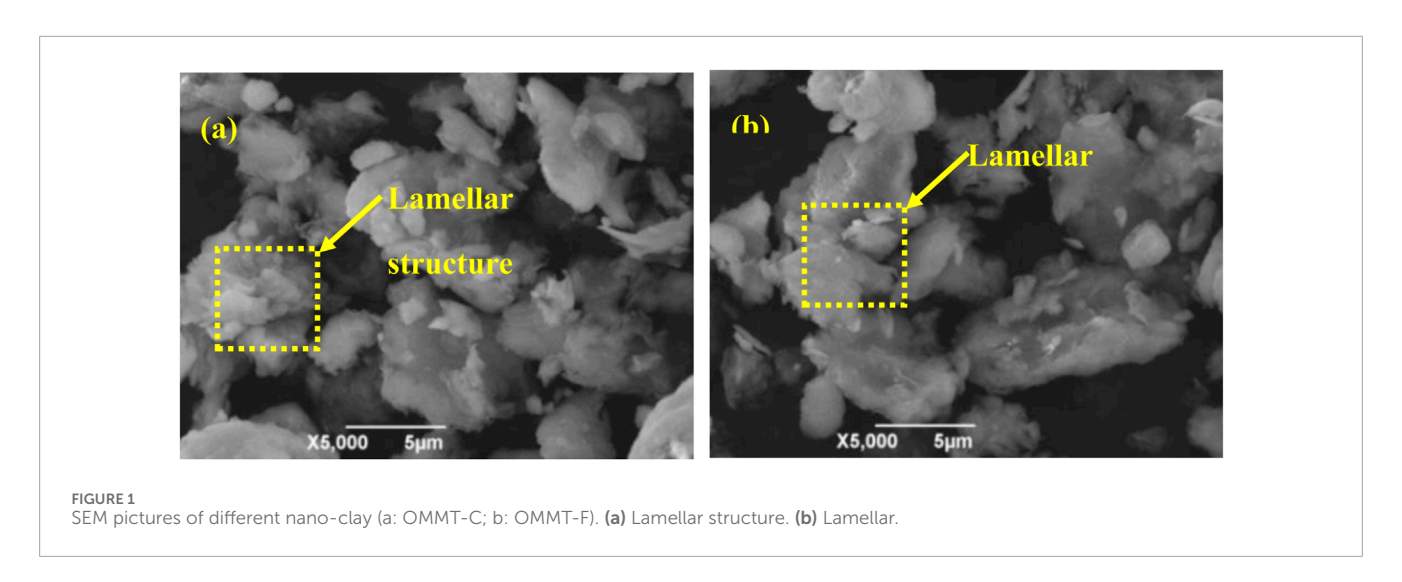
TABLE 2 Chemical composition analysis of different nano-clays.

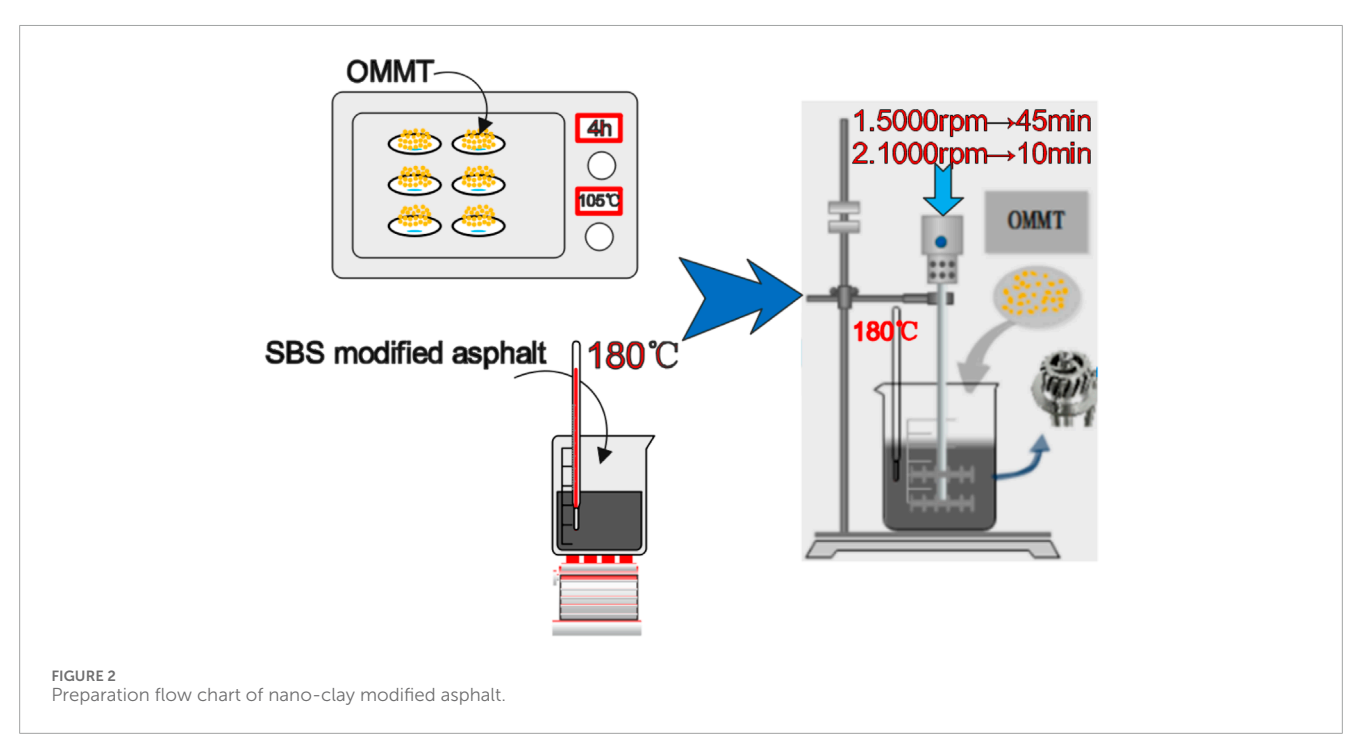
Chemical composition	OMMT-C (%)	OMMT-F (%)			
SiO ₂	71.3503	72.2106			
Al_2O_3	18.5338	19.1581			
MgO	3.0547	3.1107			
Fe ₂ O ₃	2.7701	2.2152			
K ₂ O	1.3007	0.7844			
CaO	1.1976	0.2504			
SO ₃	0.4658	0.9778			
Cl	0.4145	0.6003			
Na ₂ O	0.3178	0.2316			
TiO ₂	0.2814	0.203			
P_2O_5	0.2371	0.1898			
MnO	0.0348	0.0373			
${ m ZrO_2}$	0.0149	0.0138			
ZnO	0.0115	0.0097			
SrO	0.011	0.0038			
Rb ₂ O	0.0041	0.0034			

and there is no obvious difference in the lamellar structure of the two

2.2 Sample preparation of modified asphalt

Two kinds of nano-clay (OMMT-C and OMMT-F) with different particle sizes were selected as modifiers and SBS modified asphalt was used as reference asphalt to prepare nano-clay modified asphalt in laboratory. According to the current research, the content of nano-clay in modified asphalt is generally no more than 7%. Therefore, to consider the effect of nano-clay modifier content on asphalt performance, this paper selects different OMMT content (1%, 3%, 5% and 7%) to prepare OMMT/SBS modified asphalt. The preparation process of nano-clay modified asphalt is referred to Figure 2.





2.3 Test methods

1. Traditional performance test

This part mainly tests the penetration, softening point and ductility of asphalt binder. The testing process is mainly based on the "Standard Test Methods of Bitumen and Bituminous Mixtures for Highway Engineering" (JTG E20-2011).

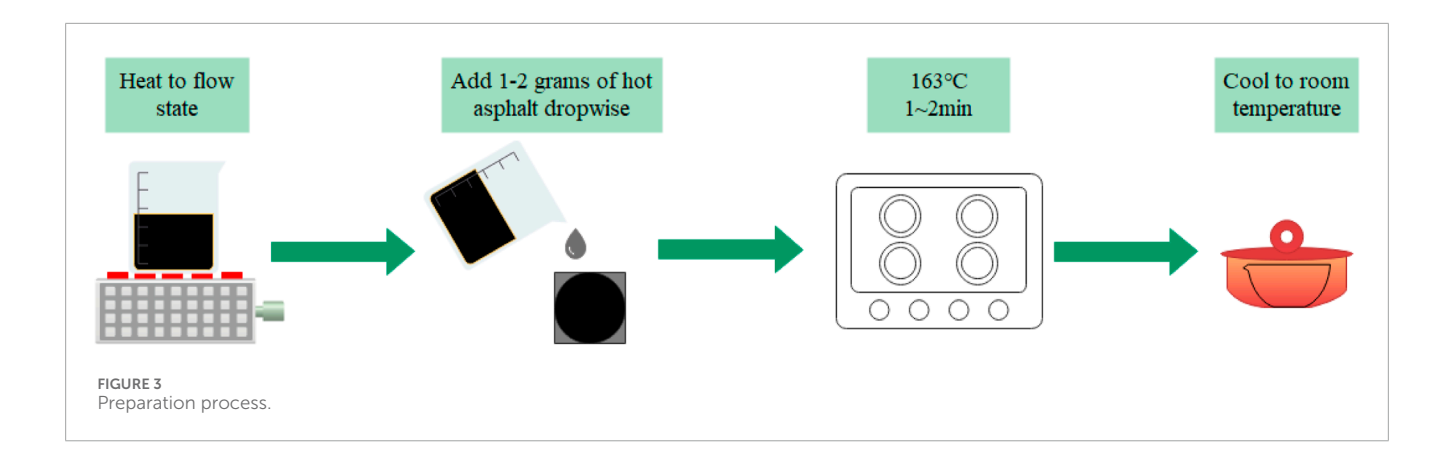
2. Temperature sweep test

To evaluate the high temperature stability of asphalt, Dynamic Shear Rheometer (DSR) is usually used to characterize the viscous and elastic properties of asphalt binder by measuring the complex shear modulus (G*) and phase angle (δ) of asphalt. The rutting factor G*/sin δ can reflect the combined influence of G*and δ at the same time.

Tests were performed using a dynamic shear rheometer, including dynamic temperature scanning, dynamic frequency scanning, and MSCR tests. Parallel plates were tested with a diameter of 25 mm and a spacing of 1 mm, with a controlled frequency of 1.59 Hz, i.e. 10 rad/s. The temperature range was from 52 °C to 84 °C, with a temperature gradient of 6 °C, with a spacing of 1 mm. The temperature range was 52 °C–84 °C with a 6 °C gradient (Li et al., 2019).

3. Fourier Transform Infrared Spectrometer (FTIR)

FTIR is the most widely used testing method for qualitative and quantitative analysis of organic polymer materials such as asphalt. The characteristic peaks and functional groups of modified asphalt can be measured by FTIR, so as to analyze its modification mechanism. In this study, the characteristic peaks and functional



groups of nano-clay OMMT-modified asphalt were scanned and quantitatively characterized by FTIR test method (model: Thermo fisher Nicolet iS10). The test range is 4,000–400 cm⁻¹. During testing, the sample is pressed into a transparent thin film using the compression method, which is then placed in the optical path. The compression method is known as the transmission mode, which is one of the most commonly used FTIR operation modes. In this mode, infrared light passes through the sample and is received by the detector to measure the absorption of infrared light by the sample.

4. Atomic force microscope test (AFM)

In this study, the surface morphology of modified asphalt were quantitatively characterized by atomic force microscope (model: Dimension Icon) of Bruke Company of the United States. The preparation of asphalt samples: drip 1-2 g of hot asphalt onto a $10 \text{ mm} \times 10 \text{ mm}$ glass slide, create a temperature environment of 163 °C using an oven, and place the hot asphalt sample horizontally. The high temperature environment makes it easy for the asphalt to obtain a flat asphalt surface. Then, take out the sample and cool it to room temperature in a drying vessel. Note that all asphalt samples are made under the same test conditions to reduce the impact of changes in test conditions on the test results. During testing, Bugdet Sensors Tap300 Al-G probe was used with an elastic constant of 3 N/m, a scanning frequency of 1.0 Hz, a scanning range of 20 um x 20 um, and a resolution of 512 x 512. All the images were collected under the peak force mode (Peak Force Quantitative Nano-Mechanics, PF-QNM) at 25 °C, and their microstructure was analyzed in detail by Nano Scope Analysis software (Ouyang et al., 2022).

The test sample preparation process is shown in Figure 3.

3 Results and discussion

3.1 Analysis of physical performance test

3.1.1 Routine performance test results

The three indexes results of different OMMT-modified asphalts are shown in Figure 4.

The influence of OMMT on modified asphalt is evident in Figure 4. The impact of two types of OMMT on the three indices of SBS modified asphalt is consistent. Specifically, as

the content of the OMMT modifier increases, there is a concurrent decrease in the penetration and ductility of the modified asphalt, coupled with an increase in the softening point.

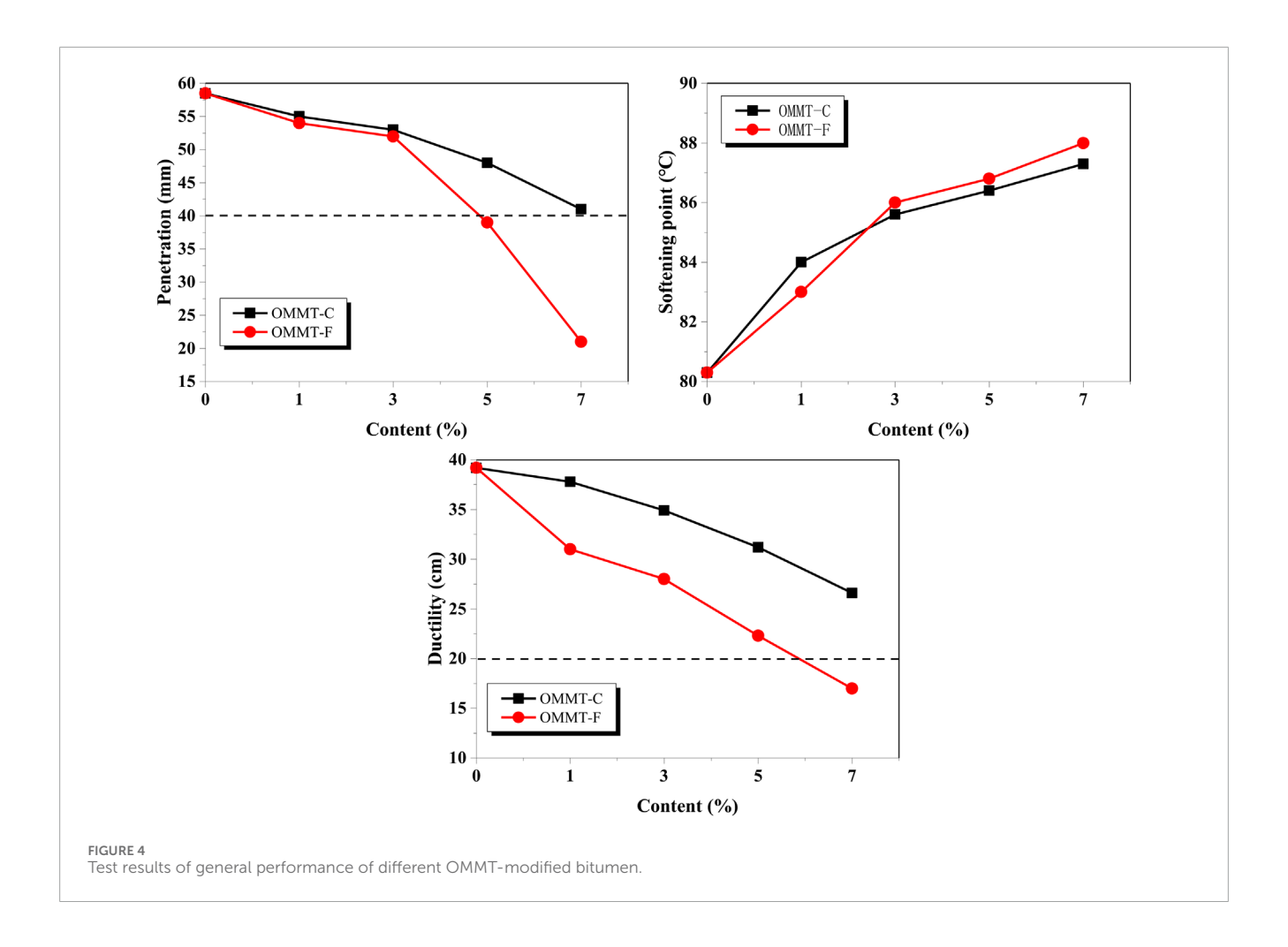
Furthermore, it is noteworthy that the impact of OMMT-F on the performance of modified asphalt surpasses that of the OMMT-C modifier significantly. Below an OMMT content threshold of 3%, the penetration test results for both modified asphalts exhibit similarity. However, beyond this threshold, particularly when the OMMT content exceeds 3%, the penetration of OMMT-F modified asphalt experiences a rapid decline. By the time the OMMT content reaches 5%, the penetration value is less than 40 mm.

The results of the ductility test for the modified asphalt exhibit a similar trend. As the OMMT content increases, the ductility of the modified asphalt undergoes a rapid decrease, with OMMT-F exerting a considerably higher influence than OMMT-C. However the changes in softening point for the two types of OMMT-modified asphalt follow an identical pattern. The softening point gradually increases with the rise in OMMT content. Specifically, when the OMMT content is below 3%, there is a significant increase in the softening point. However, beyond this threshold, particularly when the OMMT content exceeds 3%, the softening point increases at a slower rate.

The observed phenomenon may arise from the challenge of achieving uniform dispersion of excessive OMMT within SBS modified asphalt. Particularly, as the particle size of OMMT decreases, it becomes more susceptible to particle agglomeration. This agglomeration contributes to a decrease in both penetration and ductility of the modified asphalt, while the increase in softening point occurs at a slower rate.

To further analyze the reasons for this change, the internal structure of OMMT-C modified asphalt was observed by fluorescence microscopy, and the test results are shown in Figure 5.

In Figure 5, the vivid yellow particles denote SBS modifier particles. Examination of Figure 5 reveals the presence of SBS modifier particles of varying sizes within SBS modified asphalt. Upon the addition of 1% OMMT modifier, the particle size of SBS modifier decreases, fostering cross-linking among the modifier particles and establishing an effective three-dimensional network structure. This enhancement contributes to improved macroscopic performance of the modified asphalt. With the introduction of 3% OMMT modifier, the particle size of SBS modifier in the modified asphalt further diminishes, ensuring a more uniform distribution.



Conversely, at a 5% modifier content, the particle size of SBS in modified asphalt enlarges, resulting in conspicuous agglomeration. This agglomeration, in turn, contributes to the degradation of the macro performance of the modified asphalt, aligning with the outcomes of the aforementioned three indices.

The principal factor contributing to the challenge in modified asphalt lies in the propensity of nano-clay to agglomerate due to its expansive specific surface area. Additionally, the compatibility between nano-clay and asphalt is suboptimal, exacerbating the agglomeration issue. Notably, as the nano-clay content increases, the dispersion effect diminishes. From the preceding discussion, we can discern the impact of varying OMMT content on the overall three indices of modified asphalt. The micro-level elucidation of the mechanism underlying different OMMT content was conducted using fluorescence microscopy. Furthermore, a comparative analysis was performed on the overall three indices of modified asphalt with OMMT modifiers of distinct particle sizes.

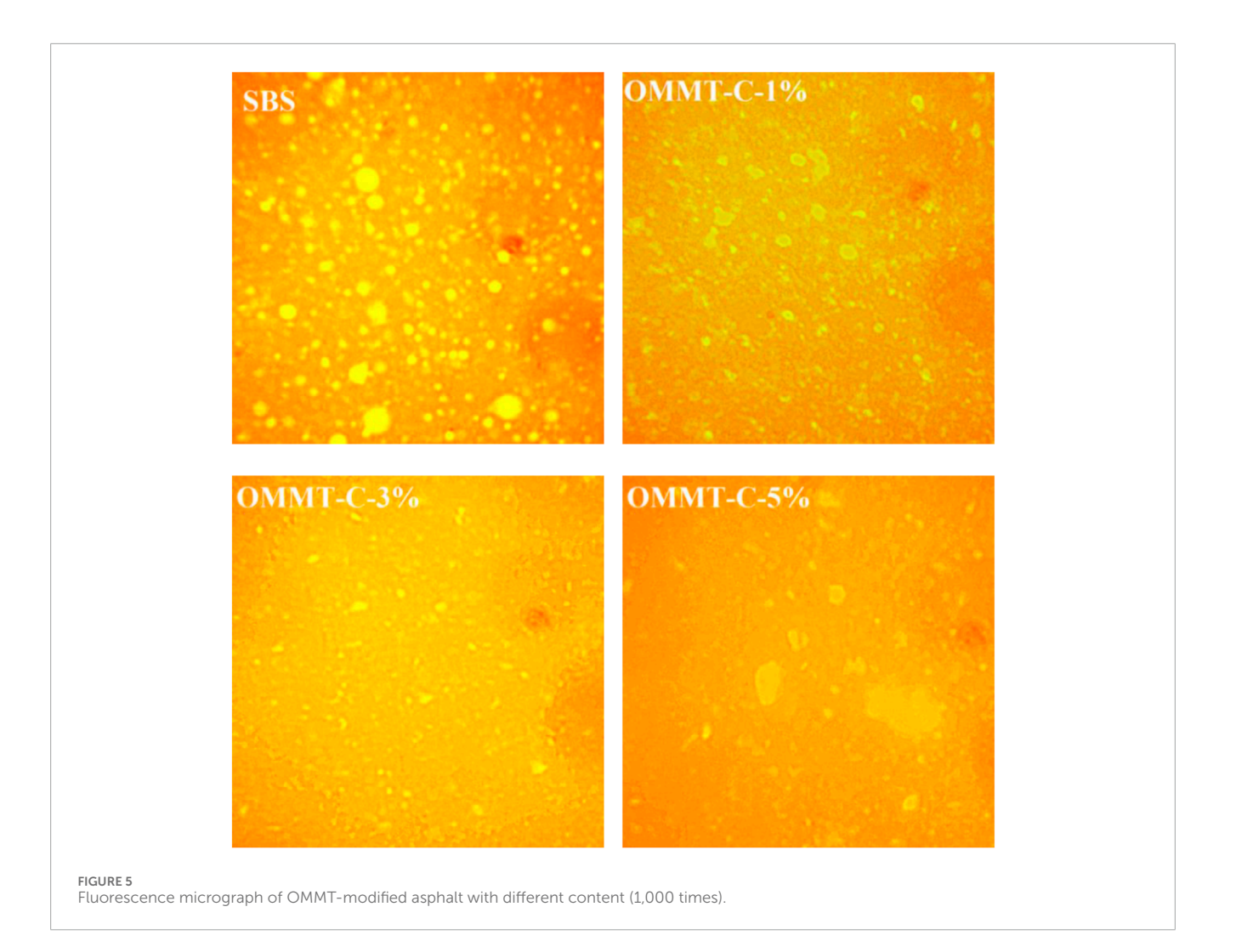
3.1.2 Temperature sweep test

The high temperature stability of different OMMT-modified asphalts was characterized by rutting factor ($G^*/\sin\delta$), and the results are shown in Figure 6. Due to a significant reduction in ductility observed at an OMMT content of 7%, adversely impacting its low-temperature performance, only OMMT-modified asphalt

with content levels of 1%, 3%, and 5% is subjected to temperature scanning tests.

Observing Figure 6, it becomes evident that the rutting factor of SBS modified asphalt exhibits negligible increase at lower OMMT content, but shows an upward trend as OMMT content rises. This observation may stem from the instability of the grid structure formed within the modified asphalt at lower OMMT content. As the OMMT content increases, a stable three-dimensional network structure is established in the modified asphalt, impeding the movement of macromolecular chains and diminishing asphalt fluidity with rising temperature. Additionally, the enhancing impact of OMMT-F on the high-temperature rheological properties of SBS modified asphalt surpasses that of OMMT-C, highlighting the influence of OMMT particle size on these properties. Specifically, OMMT with a smaller particle size can uniformly distribute within SBS modified asphalt, forming a stable three-dimensional network structure.

The introduction of OMMT modifier results in an elevation of the rutting coefficient across various temperatures. This outcome indicates that OMMT modification enhances the high-temperature deformation resistance of SBS modified asphalt, consequently improving its rutting resistance. Notably, the rutting factor for all modified bitumen exceeds 1 kPa at 82 °C. This occurrence arises from the incorporation of OMMT into the modified asphalt, leading the macromolecular chain within the asphalt to permeate the



OMMT layer. This process increases the interlayer distance, giving rise to a composite structure characterized by intercalation and exfoliation. The OMMT lamellae then form a three-dimensional network structure within the asphalt, prolonging and impeding the thermal diffusion path. This arrangement exerts a substantial blocking effect on thermal diffusion, thereby significantly enhancing the high-temperature performance of the modified asphalt.

3.2 Chemical reaction analysis of OMMT-modified asphalt

To explore the internal physical and chemical reaction mechanisms within diverse nano-clay-modified asphalts, we utilized the Fourier Transform Infrared Spectrometer (FTIR) test method. The FTIR spectrum of the modified asphalt, featuring varying OMMT content, underwent comprehensive examination. It is apparent from the preceding results that, at an OMMT content of 7%, both the penetration and ductility of the nano-modified asphalt exhibit a marked decrease. In order to comprehend the impact of different OMMT contents on the microstructure of the modified asphalt, our study conducted tests on asphalt modifications with OMMT contents of 1%, 3%, and 5%. The analysis aimed to

identify the primary characteristic peaks and functional groups of OMMT-modified asphalt. Concurrently, our investigation delved into the influence of diverse OMMT contents on the strength of characteristic peaks in the modified asphalt. A model, grounded in the relationship between OMMT content and functional group index, was established to facilitate the quantitative identification and characterization of OMMT-modified asphalt.

As shown in Figure 8, the main functional groups in the non-fingerprint zone of SBS modified asphalt are at 2,921 cm⁻¹ and 2,860 cm⁻¹, both of which are caused by the stretching vibration of C—H bond in—CH₂—(Yang et al., 2015). In addition, they also include fingerprint identification zone (600~2000 cm⁻¹) characteristic peaks and functional groups as shown in Table 3.

3.2.1 Analysis of FTIR test results of OMMT-modified asphalt

The OMMT-C and OMMT-F modifiers exhibit comparable characteristic peaks and functional groups. Consequently, this study exclusively scrutinizes the Fourier Transform Infrared Spectrometer (FTIR) of the OMMT-F modifier to discern its internal physical and chemical reaction mechanism. Figure 7 illustrates the infrared spectrum of the nano-clay OMMT modifier.

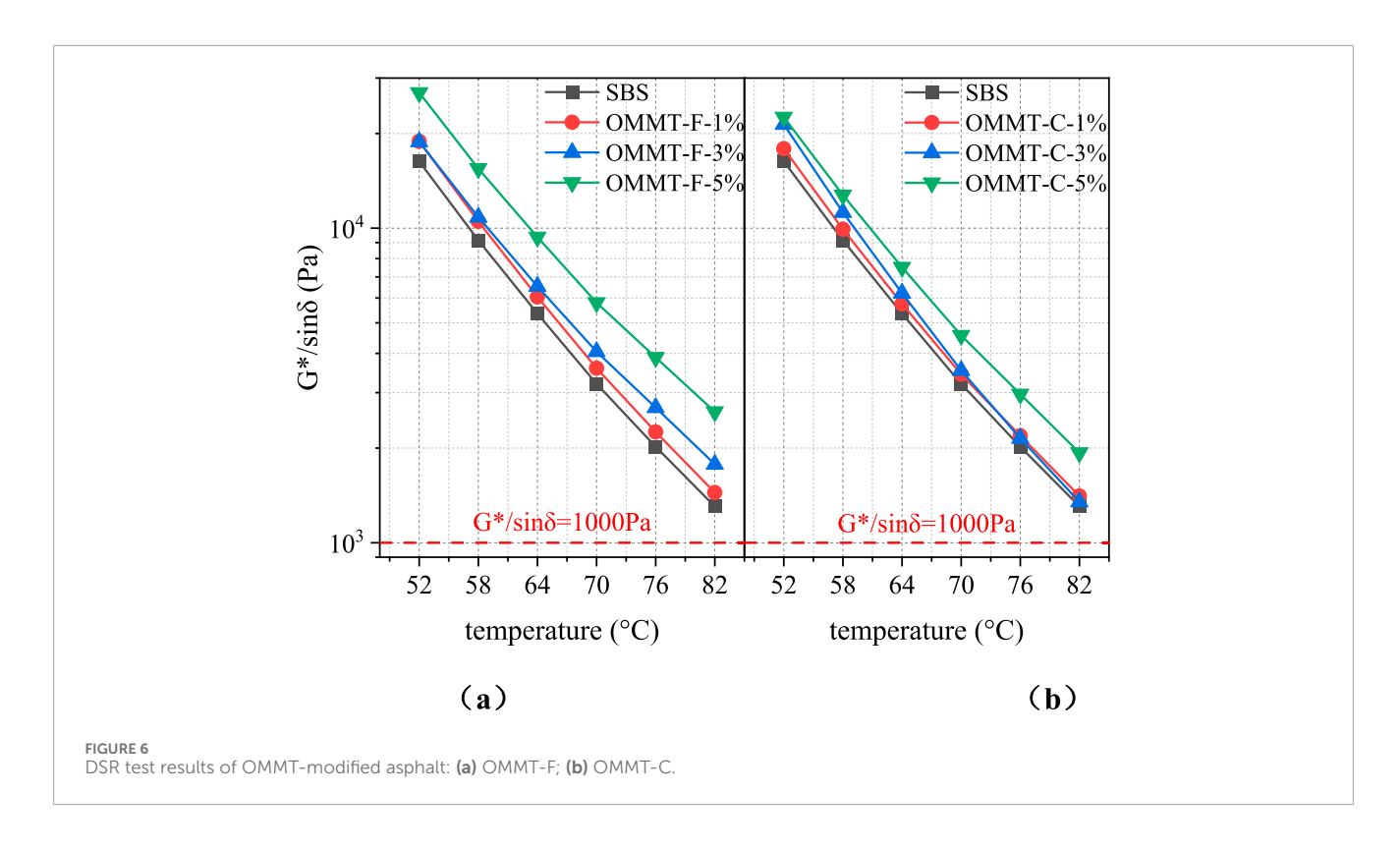


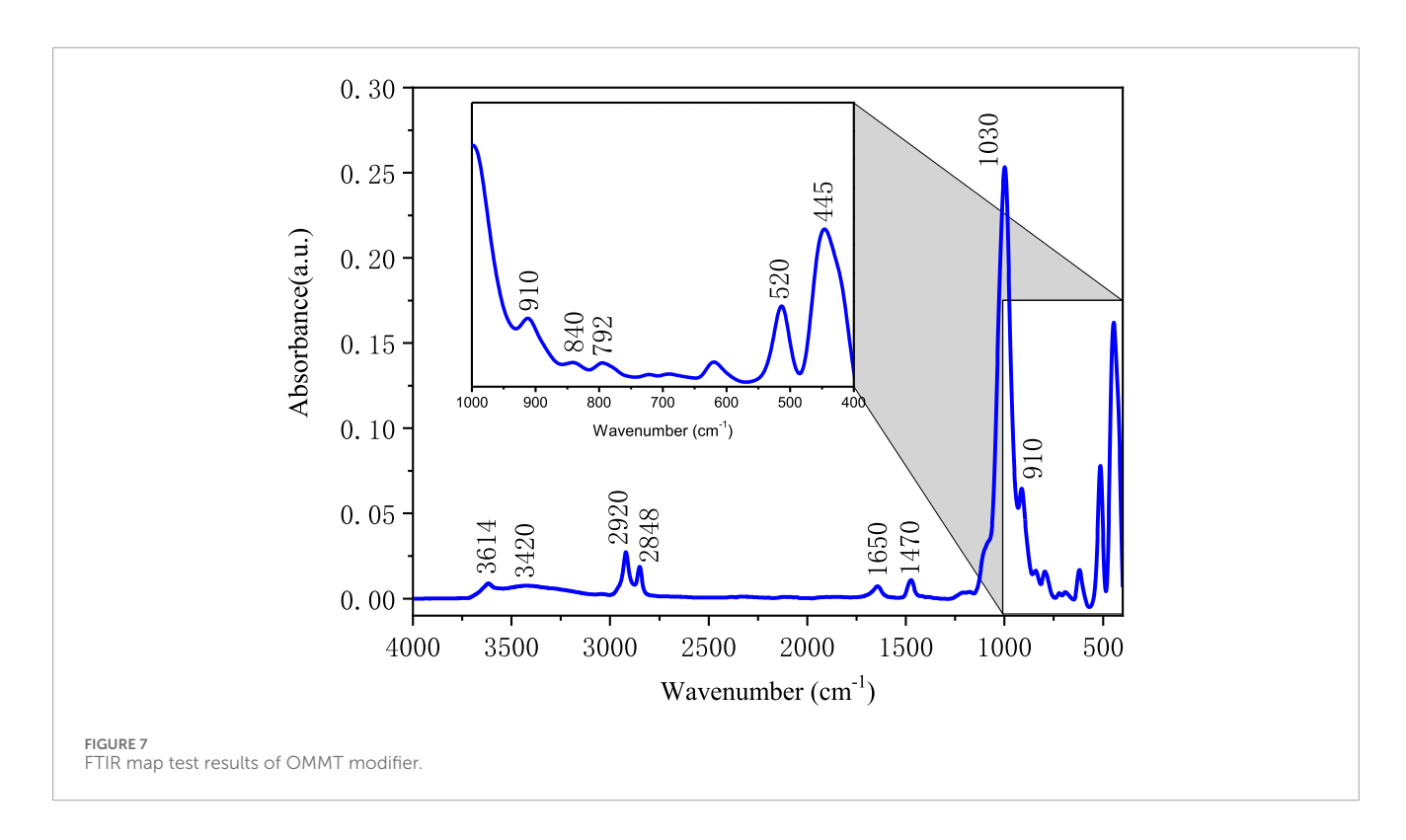
TABLE 3 Characteristic peaks and functional groups of SBS modified asphalt in the range of 600-2000 cm⁻¹ (Li et al., 2018).

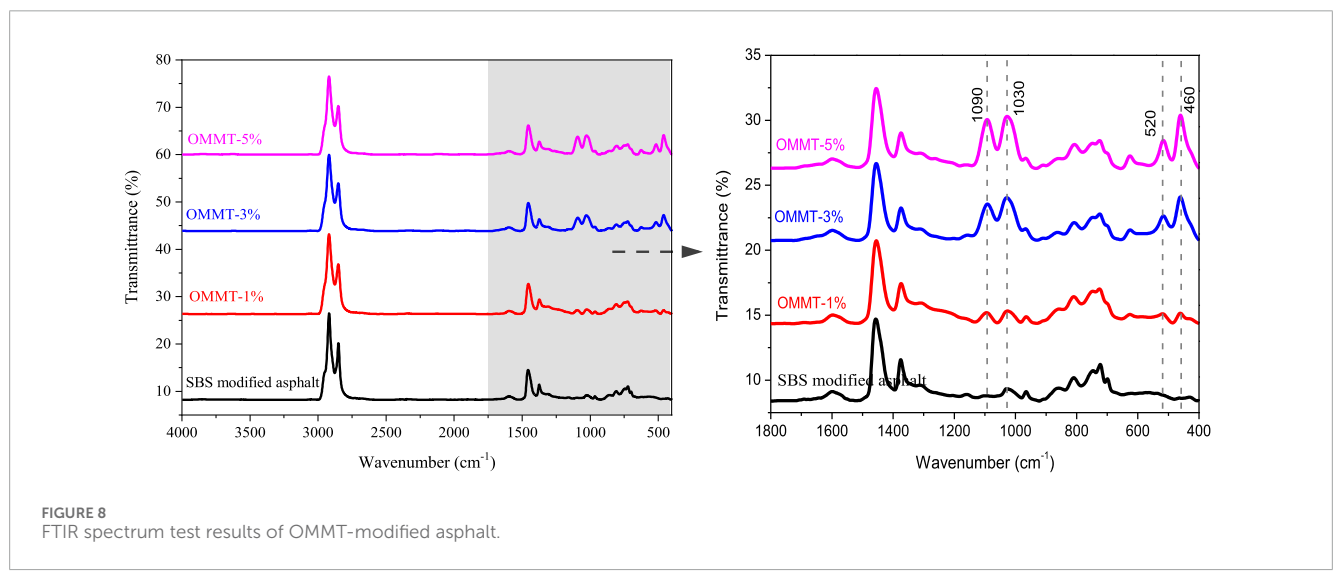
Characteristic peak/cm ⁻¹	Functional group	Characteristic peak/cm ⁻¹	Functional group		
1700	C=O	864	Stretching vibration of benzene		
1,600	C=C	814	Stretching vibration of benzene		
1,456	—СН ₂ —	743	Bending Vibration of aromatic Rings		
1,376	−CH ₃	724	$(CH_2)_n$, $(n \ge 4)$		
1,032	S=O		Bending Vibration of C-H Bond of Styren		
966	Stretching Vibration of Butadiene in SBS	700	in SBS		

As depicted in Figure 7, the peaks observed at 3,614 cm⁻¹ and 3,420 cm⁻¹ result from the bending vibration of the-OH bond. The primary origin of this functional group is attributed to the physical and chemical water molecules within the OMMT layer (Zhang H. L. et al., 2011). In the case of organically modified layered clay, the introduction of modifiers results in the presence of additional functional groups, exemplified by peaks at 2,920 cm⁻¹ and 2,848 cm⁻¹. These peaks primarily arise from the bending vibration of the C-H bond within the organic modifiers (Zhang H. L. et al., 2011; Abdelrahman et al., 2014). It also includes—OH bond tensile vibrations caused by free water and bound water between layers in layered clay, such as 1,650 cm⁻¹ and 1,470 cm⁻¹. The peak of 1,030 cm⁻¹ is the stretching vibration of Si—O bond in OMMT, and the absorption peak at $520\sim440$ cm⁻¹ is Al—O bond and Si—O bond (Zhang H. L. et al., 2011; Sikdar et al., 2008) in OMMT structure, in which 1,030 cm⁻¹ and $520\sim440~\mathrm{cm}^{-1}$ are the main characteristic peaks in OMMT modifier.

The FTIR test of OMMT-modified asphalt is carried out, and the results are shown in Figure 8.

As depicted in Figure 8, the FTIR pattern of OMMT-modified asphalt, upon the addition of OMMT, bears a resemblance to that of SBS modified asphalt. The incorporation of OMMT introduces new absorption peaks at 1,090 cm⁻¹, 1,030 cm⁻¹, 520 cm⁻¹, and 460 cm⁻¹. Comparing SBS modified asphalt and three groups of OMMT modified asphalt with different proportions, it can be found that the higher the proportion of OMMT added, the more pronounced the absorption peaks in all four directions. In comparison to Figure 7, these four absorption peaks are unique to OMMT, indicating the occurrence of specific physical and chemical reactions in OMMT-modified asphalt, resulting in the formation of new functional groups. Among them, the stretching vibration of the





Si—O bond occurs in the range of 1,100~900 cm⁻¹, while the peaks at 520 cm⁻¹ and 460 cm⁻¹ correspond to the stretching vibration of the Al—O bond and the bending vibration of the Si—O bond, respectively. These absorption peaks serve as distinctive markers for characterizing the primary characteristic peaks and functional groups of OMMT-modified asphalt. (Bin, 2010). Moreover, as the OMMT content increases, the intensity of the four absorption peaks steadily amplifies.

Compared with the FTIR spectra of OMMT modifiers, it is found that there are two peaks at $1,030~\text{cm}^{-1}$ and $1,090~\text{cm}^{-1}$ rather than a single peak $(1,030~\text{cm}^{-1})$. This is mainly due to the existence of a large number of metal cations in the montmorillonite

layer, and its strong hydration strengthens the hydrogen bond between hydroxyl and water, which weakens the absorption of Si—O bond. Thus, the absorption peaks of Si—O bond and Si—O—Si bond are combined into a single absorption peak (Jia et al., 2019). When the modifier is mixed into asphalt, with the intercalation of asphalt macromolecules, the effect of metal cations on the skeleton structure of $[Si_4O_{10}]_n$ in OMMT becomes smaller. The symmetry of silicon-oxygen tetrahedron weakens, and the absorption of Si—O and Si—O—Si is enhanced, which makes the original absorption peak split and form two absorption peaks of 1,090 cm⁻¹ and 1,030 cm⁻¹ (Zhang H. L. et al., 2011; Zhang H. et al., 2011).

In summary, the addition of OMMT to modified asphalt initiates a reaction where the OMMT modifier interacts with the asphalt, generating new functional groups and characteristic peaks. The typical functional groups are mainly Si—O bond and Al—O bond, and their characteristic peaks are mainly concentrated in 460~520 cm⁻¹ and 1,010~1,055 cm⁻¹. These absorption peaks serve as crucial markers for characterizing and discerning OMMT-modified asphalt, and their intensity systematically heightens with escalating OMMT modifier content.

3.2.2 Quantitative identification of OMMT content in modified asphalt

From the analysis of Figure 8, it can be seen that the strength of the main characteristic peaks (1,090 cm⁻¹, 1,030 cm⁻¹, 520 cm⁻¹, 460 cm⁻¹) in OMMT-modified asphalt gradually increases with the increase of modifier content. In order to clarify the effect of OMMT content on the FTIR characteristic peak of modified asphalt, the functional group index is used to evaluate the effect of modifier content on the characteristic peak, and the functional group index of characteristic peak is calculated as shown in Formula 1–5.

$$I_{1090} = AR_{1090} / \sum AR_{400-2000} \tag{1}$$

$$I_{1030} = AR_{1030} / \sum AR_{400-2000} \tag{2}$$

$$I_{520} = AR_{520} / \sum AR_{400-2000} \tag{3}$$

$$I_{460} = AR_{460} / \sum AR_{400-2000} \tag{4}$$

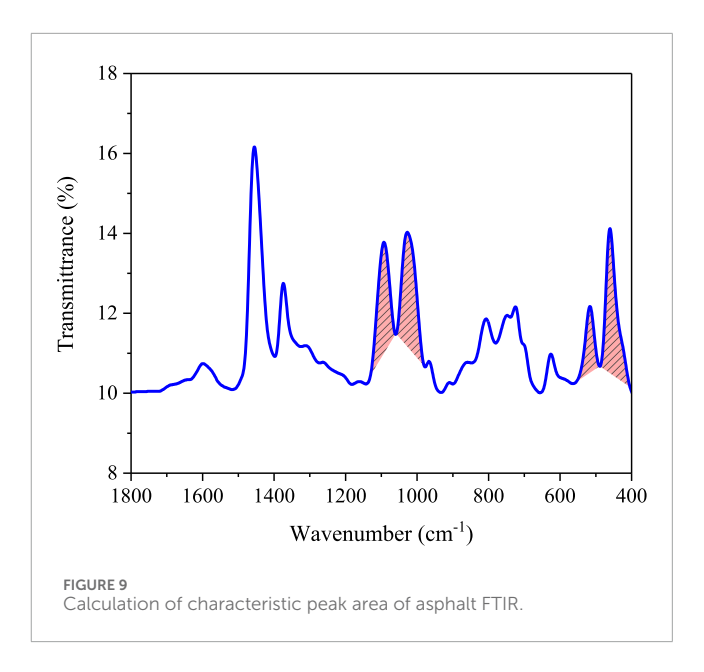
$$\sum I = I_{1090} + I_{1030} + I_{520} + I_{460} \tag{5}$$

Among them, I_{1090} , I_{1030} , I_{520} and I_{460} are the functional group indices at 1,090 cm⁻¹, 1,030 cm⁻¹, 520 cm⁻¹ and 460 cm⁻¹, respectively. AR_{1090} , AR_{1030} , AR_{520} and AR_{460} are the peak areas at 1,090 cm⁻¹, 1,030 cm⁻¹, 520 cm⁻¹ and 460 cm⁻¹, respectively. $\sum AR_{400-2000}$ is the sum of the areas of all the characteristic peaks in the 2000~400 cm⁻¹ range. $\sum I$ is the sum of the characteristic peak functional group index of OMMT-modified asphalt.

The FTIR peak area of OMMT-modified asphalt is calculated as shown in Figure 9, that is, the area surrounded by each peak curve and the baseline at both ends of the peak. Table 4 shows the calculation results of the main characteristic peak area and functional group index of different OMMT-modified asphalts.

It can be seen from Table 4 that the typical characteristic peaks represented by $1,090~\rm cm^{-1},\ 1,030~\rm cm^{-1},\ 520~\rm cm^{-1}$ and $460~\rm cm^{-1}$ are generated by the two kinds of OMMT-modified asphalt. And through the calculation of the functional group index of each characteristic peak, it is known that the calculation results of each functional group index of the two kinds of modified asphalt are similar. The particle size of nano-modifier has little effect on the degree of chemical reaction in modified asphalt. And with the increase of modifier content, the calculated value of each functional group index increases gradually. The curve of the relationship between the sum of each functional group index ($\sum I$) and the content of OMMT modifier is shown in Figure 10.

As can be seen from Figure 10, with the increase of the content of OMMT modifier, the functional group index increases gradually.



There is a good linear relationship between them, and the correlation coefficient is more than 0.96. In addition, the calculated results of the sum of the functional group indexes of the two modified asphalts are very close, and the linear fitting results are basically the same. It further shows that the particle size of OMMT modifier has little effect on the degree of chemical reaction in the modified asphalt.

Based on the above analysis, when OMMT-modified asphalt is used in production in the future, modified asphalt can be identified by four typical characteristic peaks of 1,090 cm⁻¹, 1,030 cm⁻¹, 520 cm⁻¹ and 460 cm⁻¹. And the relationship between the sum of the four typical functional group indexes and the content can be used to quantitatively characterize the OMMT modifier content of the modified asphalt. So as to provide reliable technical means for the production, use and detection of OMMT-modified asphalt.

3.3 Analysis of surface morphology of OMMT-modified asphalt

3.3.1 Micro-morphology analysis of OMMT-modified asphalt

In order to assess the impact of varying particle sizes of OMMT modifiers on asphalt micro-morphology, an Atomic Force Microscopy (AFM) test was employed to scrutinize the microstructure of the modified asphalt. Since the operational mechanisms of different quantities of OMMT modifiers on the micro-morphology of the asphalt surface are akin, we opted for comparative analysis using 1% OMMT-modified asphalt. The two-dimensional and three-dimensional topographies of the modified asphalt are depicted in Figures 11–13. Notably, the OMMT-modified material significantly alters the surface morphology of the asphalt, exhibiting distinct microstructures across different modified bitumen surfaces.

Figure 11 shows the AFM topography of SBS modified asphalt. As can be seen from Figure 11, according to the difference of color depth, there are obvious two-phase structure (such as 2D

TABLE 4 Calculation results of FTIR peak area and functional group index of modified asphalt.

Asphalt type	$\sum AR_{400-2000}$	AR ₁₀₉₀	AR ₁₀₃₀	AR ₅₂₀	AR ₄₆₀	I ₁₀₉₀	I ₁₀₃₀	I ₅₂₀	I ₄₆₀	$\sum I$
OMMT-F-0%	369.9	2.2	21.2	0.0	0.0	0.006	0.057	0.000	0.000	0.06
OMMT-F-1%	449.4	26.0	35.0	15.8	12.1	0.058	0.078	0.035	0.027	0.20
OMMT-F-3%	649.3	60.5	89.8	27.0	51.2	0.093	0.138	0.042	0.079	0.35
OMMT-F-5%	793.5	102.3	127.4	45.5	70.3	0.129	0.161	0.057	0.089	0.44
OMMT-C-0%	369.9	2.2	21.2	0.0	0.0	0.006	0.057	0.000	0.000	0.06
OMMT-C-1%	430.0	19.1	31.2	11.4	19.2	0.044	0.073	0.027	0.045	0.19
OMMT-C-3%	541.3	47.1	74.5	22.7	39.9	0.087	0.138	0.042	0.074	0.34
OMMT-C-5%	665.4	77.0	125.2	40.7	66.7	0.116	0.188	0.061	0.100	0.47

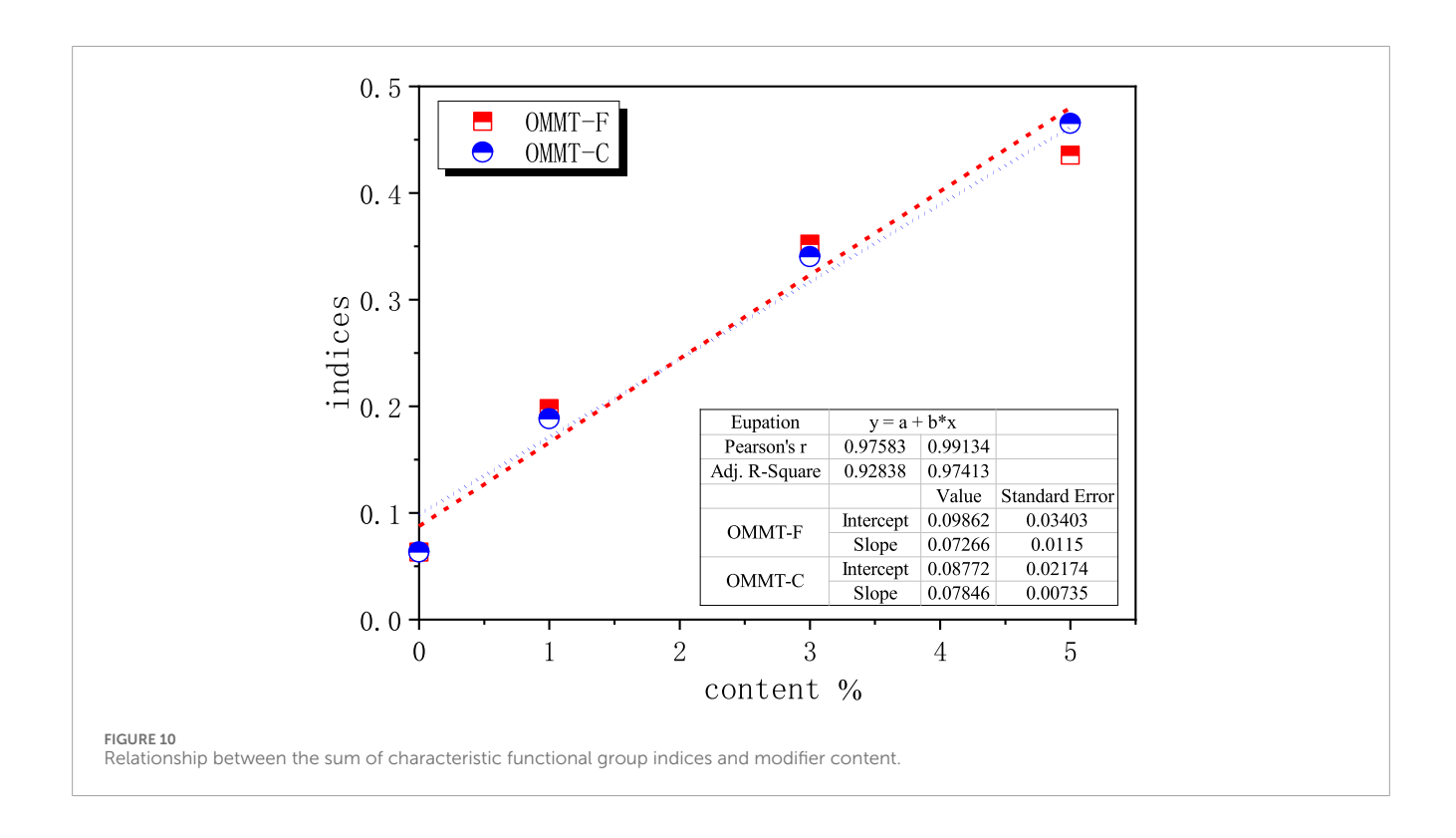
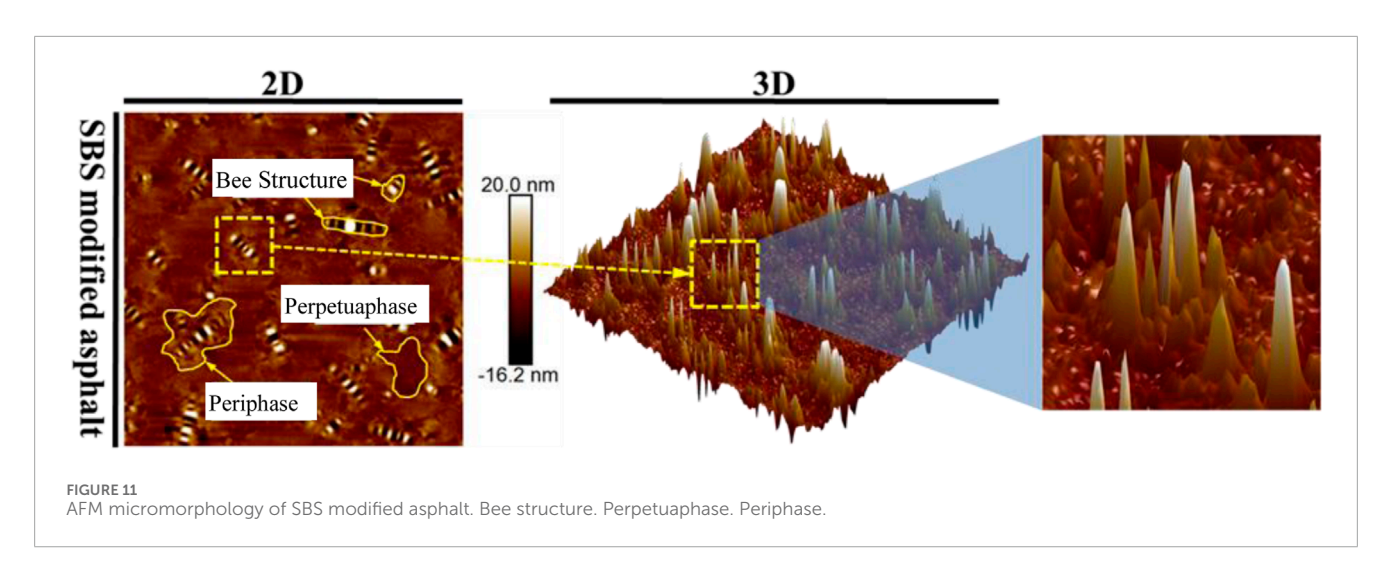


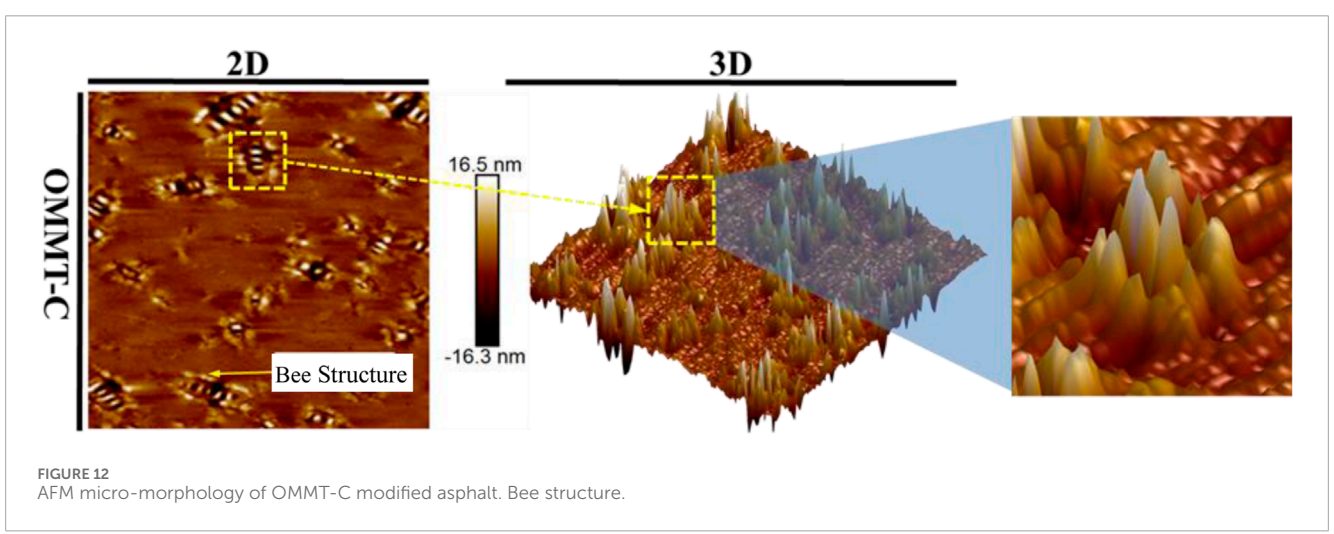
diagram) in the micro-morphology of SBS modified asphalt, that is, perpetuaphase and periphase (Xing et al., 2022). The color of perpetuaphase is darker and its height is lower, while the color of periphase is brighter, its height is higher than that of perpetuaphase. And the demarcation between the two phases is relatively obvious. According to the petroleum asphalt colloid theory, the asphalt material is divided into four components: asphaltene as the periphase, saturation and aromatics as the dispersion medium (perpetuaphase), and resins as the catanaphase to make the asphaltene uniform in the dispersion medium (Henglong, 2011). Therefore, asphalt has obvious two-phase structure.

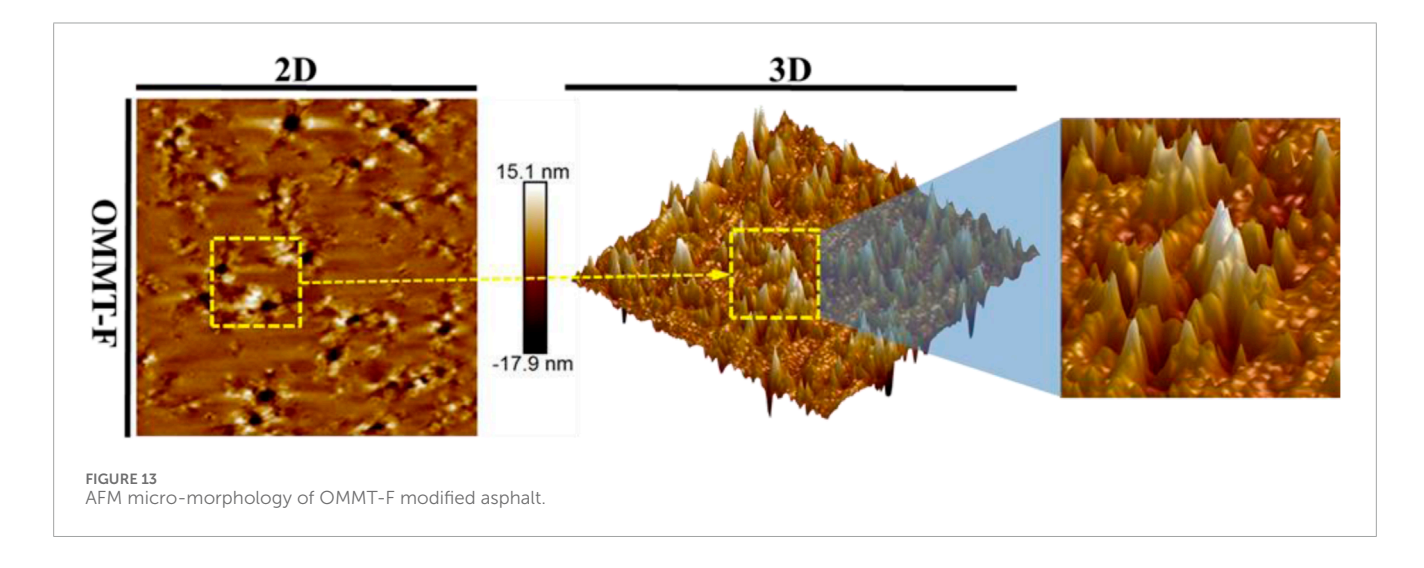
In addition, the interior of the periphase also contains areas with fluctuations in light and shade, called "bee structure". A large

number of studies have shown that the formation of bee structure is mainly due to the cooling process from high temperature to room temperature during the preparation of AFM asphalt samples. In this cooling process, the wax components (mainly microcrystalline wax) in the asphaltene will precipitate with the asphaltene, and the asphaltene will be used as the crystal nucleus to form crystals and precipitate out, and finally form a bee structure and distribute in the whole asphalt system (Dehouche et al., 2016; Li et al., 2010). There are bee structures of different sizes in SBS modified asphalt. It can be seen from the 3D diagram that these bee structures are evenly distributed in the asphalt system.

Figure 12 shows the AFM test results of OMMT-C modified asphalt. When OMMT-C modifier is added to SBS modified asphalt,







it can be seen from the 2D shape diagram that the proportion of perpetuaphase region in OMMT-C modified asphalt is significantly lower than that in SBS modified asphalt, and the addition of OMMT reduces the contrast of the two phases. The reason may be that

the molecules of the modified MMT show non-polar properties. The saturated and aromatic components are the weakest polarity components in the four components of asphalt. It is inferred from the similar compatibility principle that OMMT is more easily

dispersed among them than asphaltenes and resins, which can significantly improve the stiffness of the perpetuaphase (saturated and aromatic). So that the overall morphology of the modified asphalt tends to the development of single-phase system. In addition, compared with the SBS modified asphalt, the number of bee structure on the micro-surface of modified asphalt is reduced, and the difference between them is also reflected in the shape of the bee structure. The length and height of bee structure in OMMT-C modified asphalt decreased, but its width increased (as shown in the magnification effect of 3D diagram). At the same time, new peaks of protuberance were added on both sides of bee structure. This may be due to the formation of the intercalation structure to improve the compatibility between OMMT and asphalt materials, so that the matrix forms a more stable system. The overall stiffness of OMMT-modified asphalt is improved, which restricts the longitudinal development of crystal nucleus, affects the height of bee structure, and makes its growth direction develop horizontally.

All these show that the nano-clay OMMT-modified materials have obvious strengthening effect on the interior of the asphalt, so as to prevent the molecular chain migration of the modified asphalt at high temperature and improve the high temperature performance of the modified asphalt.

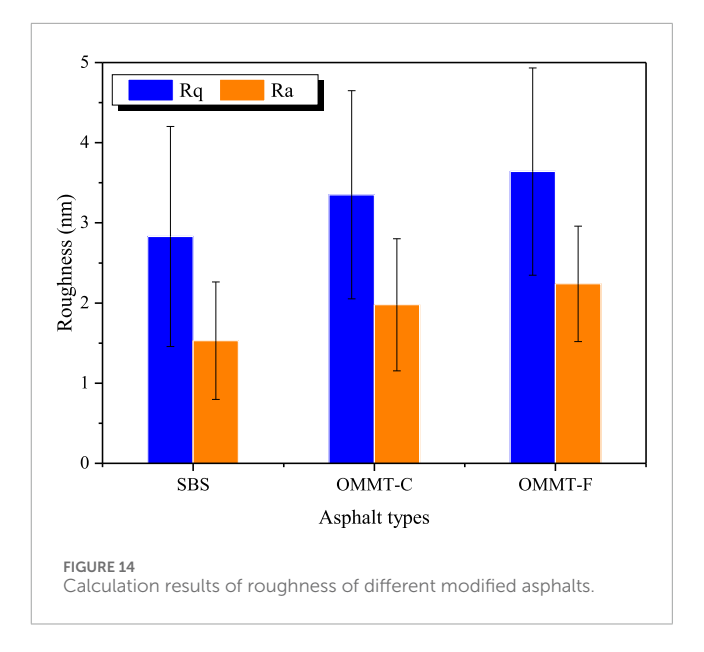
When OMMT-F modifier is added to SBS modified asphalt, the 2D shape diagram shown in Figure 13 shows that compared with OMMT-C modified asphalt, the single-phase system of OMMT-F modified asphalt is more obvious, indicating that OMMT-F modifier has better compatibility with modified asphalt. In addition, it can be seen from the 2D topography that the bee structure of the matrix surface changes to bright and dark "spots" distributed in the modified asphalt system, the reason is that OMMT dispersed in the asphalt binder as a nucleating agent is conducive to the heterogeneous nucleation of asphaltene. The surface of OMMT can absorb microcrystalline asphaltene, thus changing the morphology of the bee structure in the asphalt cooling process (Zhang and Jia, 2019). And it can be seen from the three-dimensional morphology diagram that compared with OMMT-C modified asphalt, the bee structure in OMMT-F modified asphalt is finer and the peak size is gradually smaller. This may be due to the formation of the exfoliation structure, which is beneficial to the uniform distribution of OMMT in the modified asphalt system, and further promotes the singlephase of the system. And then improve the overall stiffness of the matrix, increase the difficulty of the longitudinal development of the bee structure, so that its growth towards the horizontal development.

These micrographs show that the blocking effect of OMMT modifier on the movement of asphalt molecular chain is more obvious, and the influence on the precipitation process of bee structure is also greater, resulting in a significant decrease in the size of bee structure. The addition of modifiers increases the modulus of the asphalt surface and improves its viscoelasticity.

3.3.2 Quantitative analysis of microstructure of OMMT-modified asphalt

1. Analysis of surface roughness of modified asphalt.

To accurately analyze the changes in the microstructure of different modified asphalt, a roughness index was used to quantitatively analyze the surface morphology of different modified



asphalt (OMMT content of 1%). Roughness refers to the height difference between the high and low fluctuations in the tested area of a sample. Commonly used evaluation indicators include average roughness (Ra) and root mean square roughness (Rq). The average height value of the high and low fluctuations in the tested area and the arithmetic mean value of the average height change of $R_{\rm q}$ can both quantitatively characterize the evaluation indicators of asphalt microstructure changes. Generally, Ra values are higher than $R_{\rm q}$, and the higher the roughness value, the greater the morphological fluctuations indicated by the sample. The definitions of them are shown in Formula 6 and Formula 7.

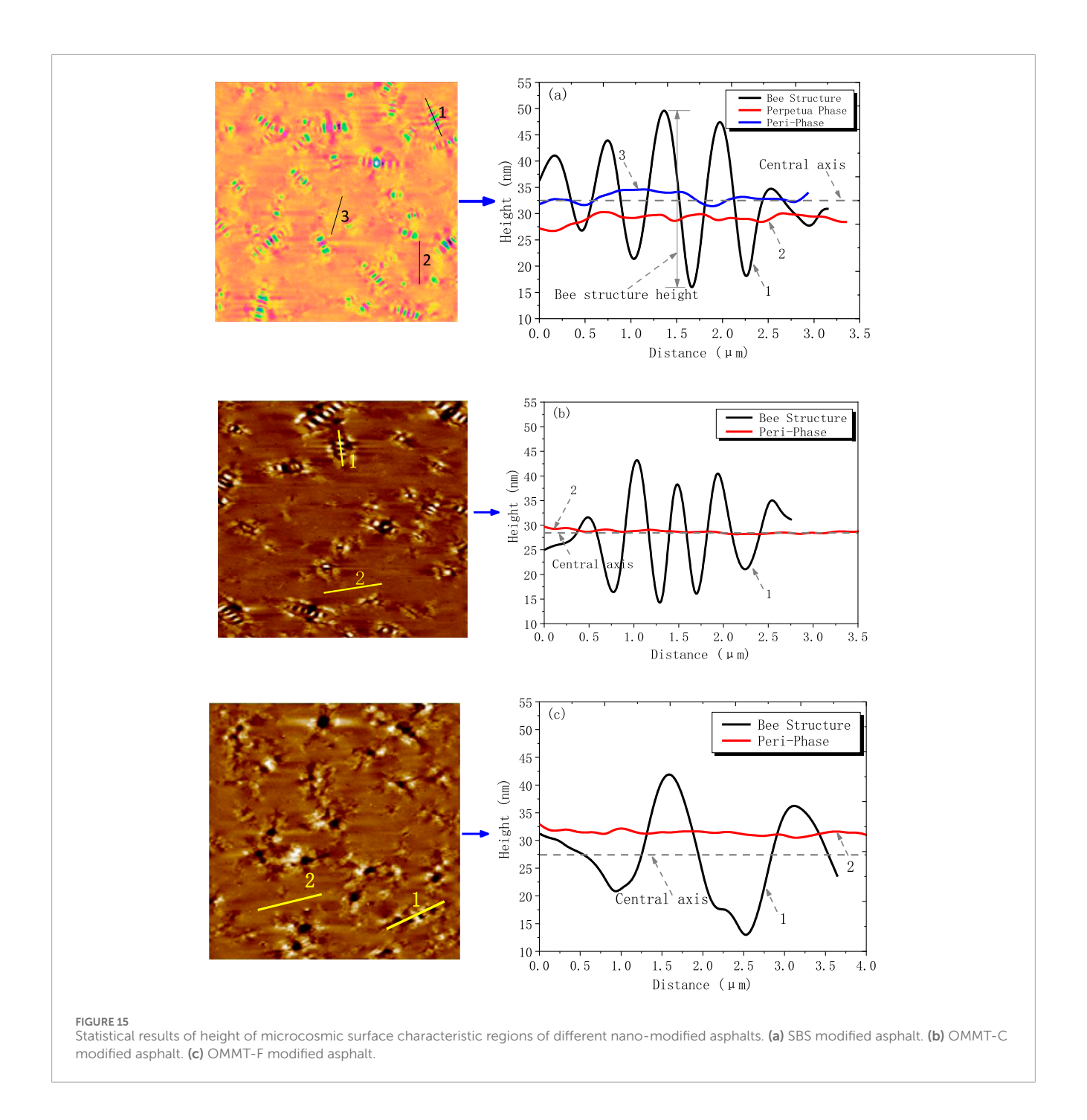
$$R_{a} = \frac{1}{N} \sum_{i}^{N} Z_{j} \tag{6}$$

$$R_q = \sqrt{\frac{\sum (Z_j)^2}{N}} \tag{7}$$

Where Z is the height of the measuring points on the surface of the sample, and N is the number of measuring points in the test area.

Formula 6 and Formula 7 are used to calculate the roughness of different modified asphalts, and the results are shown in Figure 14, where the error rod reflects the discreteness of the roughness in the test area.

It can be seen from Figure 14 that the calculation results of the two kinds of roughness show similar changes. That is, with the addition of OMMT modifier, the surface roughness of asphalt increases, and the fluctuation of surface morphology of modified asphalt increases. This is consistent with the research results of Zhang et al. (2018). The main reason is that the intercalation or exfoliation structure is formed in the OMMT-modified asphalt, and the nano-modifier has good compatibility with the asphalt. OMMT modifier acts on the perpetuaphase and periphase in the asphalt system, which makes the asphalt develop to a single-phase system (Ma et al., 2025; Fu et al., 2025; Hou et al., 2025); OMMT itself can be used as a nucleating agent, which contributes to the heterogeneous nucleation of asphaltene, thus reducing the size of the bee structure and improving the dispersion of the bee structure in the asphalt



system, so that the modified asphalt has a more stable internal structure.

2. Statistical analysis of microcosmic surface characteristic region height of modified asphalt.

The height changes of characteristic areas (perpetuaphase, periphase and bee structure) in the AFM topography of different modified asphalts are statistically analyzed, in which the content of nano-clay OMMT is 1%. The results are shown in Figure 15, where Fig. s (a), (b) and (c) represent SBS, OMMT-C and OMMT-F modified asphalt, respectively. The marker position in the left shape diagram in Figure 15 is the selected representative area. On

the right are the statistical results of the height values of each typical region.

The statistical results of the height of the characteristic areas of SBS modified asphalt are shown in Figure 15a. It can be seen from the Fig. that the height statistical results of the three characteristic areas of SBS modified asphalt are different. The average height of the perpetuaphase is about 28 nm, the average height of the periphase is about 32 nm, the height of the bee structure shows the law of fluctuation, and the maximum height of the bee structure is about 35 nm. Taking the median height of the bee structure as the central axis, it can be found that the height of the central axis is higher than

that of the perpetuaphase, and its height basically coincides with the height of the periphase.

The statistical results of the characteristic region height of OMMT-C modified asphalt are shown in Figure 15b. It is obvious from the Fig. that with the addition of OMMT-C modifier, the modified asphalt develops to single-phase system, and the proportion of perpetuaphase in the morphology diagram decreases significantly, and the test range is mainly composed of periphase and bee structure. The maximum height of bee structure is about 29 nm, which is significantly lower than that of SBS modified asphalt, which is consistent with the observation results in the above-mentioned three-dimensional topography. The average height of the periphase region of OMMT-C modified asphalt is about 30 nm, and its height coincides with the position of the central axis. Although the height of periphase is slightly lower than that of SBS modified asphalt, the overall height of OMMT-C modified asphalt is higher than that of SBS modified asphalt because of the decrease of the proportion of perpetuaphase region. This indicates that its surface modulus is higher and its viscoelasticity is improved.

When OMMT-F modifier is added to SBS modified asphalt, the height change law of the characteristic area of modified asphalt is shown in Figure 15c. Compared with SBS modified asphalt and OMMT-C modified asphalt, OMMT-F modified asphalt completely presents a single phase system. The height of the surface increases further, in which the maximum height of the bee structure is 28 nm, and the average height of the periphase is 33 nm, which is significantly higher than the height of the central axis. The results show that the influence of bee structure on the overall performance of modified asphalt is weakened.

4 Conclusion

In this investigation, nano-clay OMMT was employed to enhance SBS reference asphalt, resulting in the preparation of OMMT/SBS modified asphalt. The performance of the OMMT-modified asphalt underwent scrutiny through general performance assessments and the rutting factor $G^{\ast}/\sin\delta$ test. Subsequently, the microscopic mechanism was analyzed using FTIR and AFM tests. The ensuing conclusions are drawn:

- 1. The introduction of OMMT significantly impacts the physical properties of the modified asphalt. Specifically, the reduction in penetration and ductility, along with the increase in the softening point, indicates that the modification improves the high-temperature stability of the asphalt. This enhancement is primarily attributed to the strong interaction between the nano-clay particles and the SBS modifier. Moreover, the effect of OMMT on the performance is highly dependent on both the particle size and content, with smaller particles and higher concentrations showing a more pronounced influence on the final properties.
- 2. At OMMT contents of 1% and 3%, the SBS modifier particles maintain a uniform distribution within the asphalt matrix, which promotes the formation of a stable three-dimensional network structure. This network is essential for improving the overall macroscopic performance, as it helps prevent phase separation and ensures better load-bearing capacity and

- resistance to deformation. However, when the OMMT content exceeds 3%, the resulting agglomeration of SBS particles causes a reduction in the material's performance, as this disrupts the continuity of the modifier phase and compromises the material's rheological properties.
- 3. The FTIR analysis reveals distinct absorption peaks at 1,090 cm-1, 1,030 cm-1, 520 cm-1, and 460 cm-1, which are characteristic of the OMMT incorporation into the asphalt. These peaks serve as reliable indicators for identifying the presence of nano-clay in the modified asphalt. Furthermore, the quantity of OMMT is found to have a linear correlation with the cumulative functional group indexes at these peaks, suggesting that FTIR can be used as an effective tool for the quantitative determination of OMMT content in asphalt materials.
- 4. The interaction between OMMT and the asphaltene phase in the asphalt matrix is critical in modifying its overall properties. OMMT primarily binds with the asphaltene phase, enhancing the stiffness of the modified asphalt. This interaction helps the modified asphalt approach the stiffness of the periphase, leading to a more uniform and stable structure. This behavior is responsible for the shift toward a single-phase system in the modified asphalt, which is beneficial for improving both the mechanical and thermal properties.
- 5. The incorporation of OMMT modifies the morphology of the asphalt by promoting the dispersion of asphaltenes. This process increases the overall homogeneity of the modified asphalt, preventing the aggregation of asphaltenes that could otherwise lead to undesirable heterogeneity and instability. Asphaltene dispersion plays a crucial role in enhancing the rheological properties, including the reduced viscosity and improved elasticity of the asphalt, making it more resistant to thermal cracking and rutting under traffic load.
- 6. The findings suggest that OMMT-modified asphalt with an optimal concentration (1%–3%) can significantly improve the long-term durability and performance of the material. However, it is critical to optimize the OMMT content to avoid the negative effects of excessive modifier concentration. At higher contents, the risk of phase separation and agglomeration increases, which could compromise the modified asphalt's resistance to aging and mechanical stress. Future studies should focus on investigating the long-term aging behavior of OMMT-modified asphalt and exploring ways to mitigate the effects of excessive OMMT content on material stability.

Data availability statement

The original contributions presented in the study are included in the article/supplementary material, further inquiries can be directed to the corresponding author.

Author contributions

QY: Data curation, Methodology, Validation, Writing – original draft. ZZ: Conceptualization, Data curation, Project administration,

Writing – review and editing. ST: Supervision, Validation, Writing – review and editing. CP: Investigation, Methodology, Supervision, Writing – review and editing. HR: Conceptualization, Investigation, Supervision, Writing – original draft, Writing – review and editing.

Funding

The author(s) declare that financial support was received for the research and/or publication of this article. This work was financially supported by Guangxi Key Technologies R&D Program (Grant No. GuikeAB24010355). And the authors would like to thank the reviewers of this paper for their comments and suggestions.

Conflict of interest

Author QY was employed by Guangxi Jiaotou Technology Co., Ltd.

The remaining authors declare that the research was conducted in the absence of any commercial or financial relationships that could be construed as a potential conflict of interest.

References

Abdelrahman, M., Katti, D. R., Ghavibazoo, A., Upadhyay, H. B., and Katti, K. S. (2014). Engineering physical properties of asphalt binders through nanoclay-asphalt interactions. *J. Mater. Civ. Eng.* 26 (12), 04014099. doi:10.1061/(asce)mt.1943-5533.0001017

Bin, L. (2010). Preparation, performance and modification mechanism of organomontmorillonite modified asphalt. Wuhan University of Technology Press.

Chao, W., Tingting, X., Bochao, Z., Chao, W., Tingting, X., Xiaobin, J., et al. (2022). Effect of organic-montmorillonite on rheological performance of bioasphalt composites with various oxidative aging. *Constr. Build. Mater.* 342, 127945. doi:10.1016/j.conbuildmat.2022.127945

Crucho, J., Picado-Santos, L., Neves, J., and Capitas, S. (2019). A review of nanomaterials' effect on mechanical performance and aging of asphalt mixtures. *Appl. Sciences-Basel* 9 (18), 3657. doi:10.3390/app9183657

Dehouche, N., Kaci, M., and Mouillet, V. (2016). The effects of mixing rate on morphology and physical properties of bitumen/organo-modified montmorillonite nanocomposites. *Constr. Build. Mater.* 114, 76–86. doi:10.1016/j.conbuildmat.2016.03.151

Fu, Z., Yang, P., Dai, J., Ma, F., Hou, Y., Zhu, C., et al. (2025). Rheological properties and microscopic mechanism of composite regenerated asphalt. *Fuel* 385, 134159. doi:10.1016/j.fuel.2024.134159

Henglong, Z. (2011). Preparation and properties of bitumen/inorganic nanocomposites. Wuhan University of Technology Press.

Hou, G., Tao, W., Liu, J., Zhang, X., Dong, M., and Zhang, L. (2017). Effect of the structural characteristics of solution styrene–butadiene rubber on the properties of rubber composites. *J. Appl. Polym. Sci.* 135, 45749. doi:10.1002/app.45749

Hou, Y., Ma, F., Fu, Z., Dai, J., Tang, Y., Wang, T., et al. (2025). Diffusion behavior of phase change materials at the interface of aged asphalt binder based on molecular dynamics simulation and experimental analysis. *J. Mol. Liq.* 419, 126758. doi:10.1016/j.molliq.2024.126758

Iskender, E., Aksoy, A., and Ozen, H. (2012). Indirect performance comparison for styrene–butadiene–styrene polymer and fatty amine anti-strip modified asphalt mixtures. *Constr. Build. Mater.* 30, 117–124. doi:10.1016/j.conbuildmat.2011.11.027

Jahromi, S. G., and Khodaii, A. (2009). Effects of nanoclay on rheological properties of bitumen binder. *Constr. Build. Mater.* 23 (8), 2894–2904. doi:10.1016/j.conbuildmat.2009.02.027

Jasso, M., Bakos, D., Stastna, J., and Zanzotto, L. (2012). Conventional asphalt modified by physical mixtures of linear SBS and montmorillonite. *Appl. Clay Sci.* 70, 37–44. doi:10.1016/j.clay.2012.09.004

Jia, M., Zhang, Z., Wei, L., Wu, X., Cui, X., Zhang, H., et al. (2019). Study on properties and mechanism of organic montmorillonite modified bitumens:

Generative Al statement

The author(s) declare that no Generative AI was used in the creation of this manuscript.

Any alternative text (alt text) provided alongside figures in this article has been generated by Frontiers with the support of artificial intelligence and reasonable efforts have been made to ensure accuracy, including review by the authors wherever possible. If you identify any issues, please contact us.

Publisher's note

All claims expressed in this article are solely those of the authors and do not necessarily represent those of their affiliated organizations, or those of the publisher, the editors and the reviewers. Any product that may be evaluated in this article, or claim that may be made by its manufacturer, is not guaranteed or endorsed by the publisher.

view from the selection of organic reagents. Constr. Build. Mater. 217, 331–342. doi:10.1016/j.conbuildmat.2019.05.074

Larsen, D. O., Alessandrini, J. L., Bosch, A., and Cortizo, M. S. (2009). Micro-structural and rheological characteristics of SBS-asphalt blends during their manufacturing. *Constr. and Build. Mater.* 23 (8), 2769–2774. doi:10.1016/j.conbuildmat.2009.03.008

Li, B., Zhang, H., and Yu, J. (2010). Effect of organo-montmorillonite on the morphology and aging properties of various bitumens. *J. Wuhan Univ. Technology-Materials Sci. Ed.* 25 (4), 650–655. doi:10.1007/s11595-010-0063-6

Li, Y., Wu, S., Pang, L., Liu, Q., Wang, Z., and Zhang, A. (2018). Investigation of the effect of Mg-Al-LDH on pavement performance and aging resistance of styrene-butadiene-styrene modified asphalt. *Constr. Build. Mater.* 172, 584–596. doi:10.1016/j.conbuildmat.2018.03.280

Li, B., Zhou, J. N., Zhang, Z. H., Yang, X. L., and Wu, Y. (2019). Effect of short-term aging on asphalt modified using microwave activation crumb rubber. *Materials* 12 (7), 1039. doi:10.3390/ma12071039

Liu, H., Chen, Z., Wang, W., Wang, H., and Hao, P. (2014). Investigation of the rheological modification mechanism of crumb rubber modified asphalt (CRMA) containing TOR additive. *Constr. and Build. Mater.* 67, 225–233. doi:10.1016/j.conbuildmat.2013.11.031

Liu, H., Zhang, Z., Xie, J., Gui, Z., Li, N., and Xu, Y. (2021). Analysis of OMMT strengthened UV aging-resistance of Sasobit/SBS modified asphalt: its preparation, characterization and mechanism. *J. Clean. Prod.* 315, 128139. doi:10.1016/j.jclepro.2021.128139

Ll Bo, L. P., Xin-yu, ZHANG, Gui, C. A. O., and Xiao-long, YANG (2017). Interaction and particle effect of crumb rubber characteristics on brookfield viscosity of rubber asphalt binder. *J. Chang'an Univ. Sci. Ed.* 37 (02), 26–34.

Lu, H., Ye, F., Yuan, J., and Yin, W. (2018). Properties comparison and mechanism analysis of naphthenic oil/SBS and nano-MMT/SBS modified asphalt. *Constr. Build. Mater.* 187, 1147–1157. doi:10.1016/j.conbuildmat.2018.08.067

Ma, F., Dai, J., Zou, Y., Fu, Z., Liu, J., Yang, P., et al. (2025). Preparation of low-temperature microencapsulated phase change materials and evaluation of their effect on the properties of asphalt binders. *Constr. Build. Mater.* 458, 139719. doi:10.1016/j.conbuildmat.2024.139719

Ouyang, Q. J., Xie, Z. W., Liu, J. H., Gong, M. H., and Yu, H. Y. (2022). Application of atomic force microscopy as advanced asphalt testing technology: a comprehensive review. *Polymers* 14 (14), 2851. doi:10.3390/polym14142851

Park, H. M., Choi, J. Y., Lee, H. J., and Hwang, E. Y. (2009). Performance evaluation of a high durability asphalt binder and a high durability asphalt mixture for bridge deck pavements. *Constr. Build. Mater.* 23 (1), 219–225. doi:10.1016/j.conbuildmat.2008.01.001

Ren Xiaoyu, L. B., Yongning, W., Zhihao, Z., and Yujiao, C. (2020). Impact of ultraviolet aging conditions on typical functional groups for warm-mixed SBS modified asphalt. *J. Mater. Sci. and. Eng.* 38 (06), 971–976.

- Shah, P. M., and Mir, M. S. (2020). Performance of OMMT/SBS on the rheological properties of asphalt binder. *Korea-Australia Rheology J.* 32 (4), 235–242. doi:10.1007/s13367-020-0022-5
- Sikdar, D., Katti, K. S., and Katti, D. R. (2008). Molecular interactions alter clay and polymer structure in polymer clay nanocomposites. *J. Nanosci. Nanotechnol.* 8 (4), 1638–1657. doi:10.1166/jnn.2008.18228
- Sun, L., Wang, Y., and Zhang, Y. (2014). Aging mechanism and effective recycling ratio of SBS modified asphalt. *Constr. Build. Mater.* 70, 26–35. doi:10.1016/j.conbuildmat.2014.07.064
- Tan, Z.-h., Wang, J.-j., and Shi, Z.-n. (2020). Laboratory investigation on effects of organic montmorillonite on performance of crumb rubber modified asphalt. *J. Central South Univ.* 27 (12), 3888–3898. doi:10.1007/s11771-020-4578-5
- Transport, E. D. (2013). Review on China's road engineering research: 2013. *China J. Highw. Transp.* 26 (03), 1–36.
- Wang, H., Dang, Z., Li, L., and You, Z. (2013). Analysis on fatigue crack growth laws for crumb rubber modified (CRM) asphalt mixture. *Constr. and Build. Mater.* 47 (5), 1342–1349. doi:10.1016/j.conbuildmat.2013.06.014
- Wang, D., Liu, Q., Yang, Q., Tovar, C., Tan, Y., and Oeser, M. (2019). Thermal oxidative and ultraviolet ageing behaviour of nano-montmorillonite modified bitumen. *Road Mater. Pavement Des.* 22 (1), 121–139. doi:10.1080/14680629.2019.1619619
- Wen-jun, S. L. Z. H.-R. (2013). Preparation of nano-modified asphalt and lts road performance evaluation. *China J. Highw. Transp.* 26 (01), 15–22.
- Xiao, X., and Zhang, D. (2017). Properties of montmorillonite modified asphalt modified by isophorone diisocyanate. *J. South China Univ. Technol.* 45 (02), 116–121.
- Xing, C., Jiang, W., Li, M., Wang, M., Xiao, J., and Xu, Z. (2022). Application of atomic force microscopy in bitumen materials at the nanoscale: a review. *Constr. Build. Mater.* 342, 128059. doi:10.1016/j.conbuildmat.2022.128059
- Xiong Hui, L.H.-H. (2020). Study on performance of nanocomposite-modified asphalt binder and mixture. *J. China and Foreign Highw.* 40 (04), 225–229.
- Yang, X., You, Z., and Mills-Beale, J. (2015). Asphalt binders blended with a high percentage of biobinders: aging mechanism using FTIR and rheology. *J. Mater. Civ. Eng.* 27 (4), 04014157. doi:10.1061/(asce)mt.1943-5533.0001117

- Yu, J., Zeng, X., Wu, S., Wang, L., and Liu, G. (2007). Preparation and properties of montmorillonite modified asphalts. *Mater. Sci. Eng. A* 447 (1-2), 233–238. doi:10.1016/j.msea.2006.10.037
- Yunbin, K., Jitao, C., Song, X., Chongyu, B., Chao, Z., and Xiaojuan, J. (2022). Storage stability and anti-aging performance of SEBS/organ-montmorillonite modified asphalt. *Constr. Build. Mater.* 341, 127875. doi:10.1016/j.conbuildmat.2022. 127875
- Zhang, Z., and Jia, M. (2019). Evaluating the effect of organic reagents on short-term aging resistance of the organic rectorite asphalt by multi-indicators. *Road Mater. Pavement Des.*, 215–229. doi:10.1080/14680629.2019.
- Zhang H., H., Yu, J., Wang, H., and Xue, L. (2011). Investigation of microstructures and ultraviolet aging properties of organo-montmorillonite/SBS modified bitumen. *Mater. Chem. Phys.* 129 (3), 769–776. doi:10.1016/j.matchemphys.2011.
- Zhang H. L., H. L., Yu, J. Y., Xue, L. H., and Li, Z. C. (2011). Effect of montmorillonite organic modification on microstructures and ultraviolet aging properties of bitumen. *J. Microsc.* 244 (1), 85–92. doi:10.1111/j.1365-2818.2011.03511.x
- Zhang, H., Yu, J., and Wu, S. (2012). Effect of montmorillonite organic modification on ultraviolet aging properties of SBS modified bitumen. *Constr. Build. Mater.* 27 (1), 553–559. doi:10.1016/j.conbuildmat.2011.07.008
- Zhang, H., Xu, H., Wang, X., and Yu, J. (2013). Microstructures and thermal aging mechanism of expanded vermiculite modified bitumen. *Constr. Build. Mater.* 47, 919–926. doi:10.1016/j.conbuildmat.2013.05.099
- Zhang, H., Zhu, C., Tan, B., and Shi, C. (2014). Effect of organic layered silicate on microstructures and aging properties of styrene–butadiene–styrene copolymer modified bitumen. *Constr. Build. Mater.* 68, 31–38. doi:10.1016/j.conbuildmat.2014.06.038
- Zhang, Z., Jia, M., Jiao, W., Qi, B., and Liu, H. (2018). Physical properties and microstructures of organic rectorites and their modified asphalts. *Constr. Build. Mater.* 171, 33–43. doi:10.1016/j.conbuildmat.2018.01.163
- Zhang Shuai, Z. J. (2020). Study on preparation of organic montmorillonite by freezedrying method and its modified asphalt performance. *Mater. Rep.* 34 (04), 4037–4042.
- Zhao, X., Wang, S., Wang, Q., and Yao, H. (2016). Rheological and structural evolution of SBS modified asphalts under natural weathering. *Fuel* 184, 242–247. doi:10.1016/j.fuel.2016.07.018